Lithological constraints from seismic waveforms: application to the opal-A to opal-CT transition

Mohammad Maysami[1] *and Felix J. Herrmann, University of British Columbia*

SUMMARY

In this paper, we present a new method for seismic waveform characterization whose aim is threefold, namely (i) extraction of detailed information on the sharpness of transitions in the subsurface from seismic waveforms, (ii) reflector modeling, based on binary-mixture and percolation theory, and (iii) establishment of well-seismic ties, through parameterizations of our waveform and critical reflector model. We test this methodology on the opal-A (Amorphous) to opal-CT (Cristobalite/Tridymite) transition imaged in a migrated section of North Sea field data West of the Shetlands.

INTRODUCTION

Integrating information observed from seismic waveforms to the fine details of unconformities in the subsurface has been a challenge for many years. Not only does this integration require a thorough understanding of the (rock)physics responsible for the unconformity but one also needs to come up with parameterizations, and subsequent nonlinear inversion methodologies, that capture the essence of what constitutes reflectivity and what reflector information translates into the waveforms. In this paper, we address all of these issues by presenting (i) a parametric representation for reflectors and waveforms that borrows from earlier work by the authors (see e.g. Herrmann et al., 2001; Herrmann, 2005, and the references therein), (ii) a new nonlinear estimation method for the reflector parameters, and (iii) a rock-physical model that generates transitions, consistent with the parametric model proposed by Herrmann and Bernabé (2004) to model mineralogical phase transitions at upper-mantle discontinuities.

It is well-known that seismic waves reflect specularly at regions where the elastic moduli (not necessary the density as we show below) vary significantly at the length scale proportional to the seismic wavelength. Motivated by empirical studies on sedimentary records, Herrmann et al. (2001) made the argument that reflectors can be considered as algebraic singularities, parameterized by a scaling exponent determining the transition sharpness. It was shown that this parameterization corresponds to a generalization of zero- or first-order discontinuities towards fractional-order scale-invariant transitions, indexed by a scale exponent. Ever since this generalization, scientists, including the authors, have been making efforts to extract these exponents from seismic data (Herrmann et al., 2001; Herrmann, 2001, 2005). These efforts are hampered by the fact that scale exponents are typically found by conducting a multiscale analysis, which is appropriate for broadband data such as sedimentary records. Unfortunately, migrated data is bandwidth limited and this explains the challenge. In this paper, we present the latest developments in the estimation of this important parameter through a detecting-estimation technique during which the waveforms are first located, then segmented and subsequently inverted with a nonlinear procedure.

With the estimated sharpness information, interesting questions arise, such as what is the geological and rock-physical significance of this parameterization by scale exponents? Indeed, as reported by Herrmann et al. (2001), there are indications that the proposed scale exponent correlates with changes along clinoforms that are consistent with changes in the depositional environment. Albeit insightful, in this paper we aim to answer the question at the rock-physical level by studying the behavior of binary mixtures (e.g. opal-A to opal-CT) as a function of their volume fractions. At this point one may be tempted to resort to traditional Hashin-Shtrikman (HS) or Reuss-Voigt bounds to constrain the elastic moduli (see e.g. Hashin and Shtrikman, 1962). Unfortunately, these models are smooth as a function of the volume fraction, which we will consider as a proxi for depth. This smoothness excludes sharp transitions and hence specular reflections. To counter this unsatisfactory aspect of equivalent medium theory, Herrmann and Bernabé (2004) proposed an alternative model, where the elastic moduli are predicted to change drastically as soon as a critical volume fraction for the stiffer of the two materials of the binary mixture is reached. At this critical threshold, according to this model, the stiffer of the two materials connects and the overall strength of the macroscopic rock matrix will depend on the size of the connected cluster of the strong material. As this cluster grows with a scale exponent, a cusp-like singularity is created (Herrmann and Bernabé, 2004).

In this paper, we will use this percolation model to explain the unconformity associated with the opal-A to opal-CT transition observed throughout a migrated section near the Shetland islands. Constrained by core data from a well intersecting this seismic line, we built a reflector model that generates a seismic waveform similar to the one observed from the data and hence we are providing a well tie.

Our paper is organized as follows. First, we present the parametric reflector model, followed by a parameterization-estimation technique for waveform data. Next, we briefly introduce the percolation model and discuss the type of seismic response it generates. We conclude by using this model, in conjunction with the parametric estimation, to constrain the opal-A to opal-CT transition from well and seismic data.

SEISMIC WAVEFORM CHARACTERIZATION

In this section, we present our parametric waveform inversion method consisting of a detection, segmentation, and an estimation stage.

Waveform parameterization: As proposed by Herrmann et al. (2001); Herrmann (2001), transitions in the Earth's subsurface can be modeled by algebraic singularities, parameterized by

[1]Currently at Stanford University

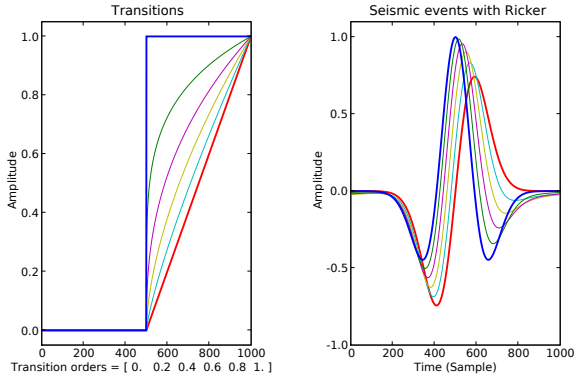

Figure 1: Generalized transition model with scale exponents varying from zero- to first-order. **(a)** Zero- (blue), first- (red), and fractional-order transitions. **(b)** Corresponding seismic waveforms, yielded by the convolution of the reflectivity with a Ricker wavelet. Notice how the reflected waveform changes from the Ricker wavelet for the zero-order transition to the integral of the Ricker wavelet for the first-order discontinuity.

a scale exponent. As can be seen from Figure 1, the corresponding waveforms yielded by the linear convolution model change significantly as a function of the singularity order. For the zero-order transition, we observe the Ricker wavelet itself, which is consistent with the fact that the reflectivity for that transition is given by the delta Dirac distribution, while for the first-order discontinuity time-integrated waveform is observed.

In all generality according to this transition model, we can consider a seismic trace as a superposition of waveforms generated by different fractional-order transitions. Mathematically, this superposition can, in the Fourier domain, be written in the following algebraic form (Blu and Unser, 2003):

$$\hat{s}(\omega) = \sum_i c_i \hat{\varphi}_{\theta_i}(\omega), \tag{1}$$

with $\hat{\varphi}_\theta(\omega) = (j\omega)^{-\alpha/2+\phi}\ (-j\omega)^{-\alpha/2-\phi}\ e^{-\frac{(\sigma^2\omega^2)}{2}}\ e^{-j\omega\tau}$, - where α is related to the singularity order, σ is the bandwidth, ϕ the phase rotation, and τ the location of the waveform (see also Herrmann, 2005, for further details). According to Equation 1, the seismic response is made out of waveforms which for each i are parameterized with $\theta_i = \{\tau_i, \sigma_i, \alpha_i, \phi_i\}$. Because the seismic trace is assumed to be linearly related to the reflectivity, the attributes of this parameterization, in particular the scale exponent α, are directly related to the order of the transition. Moreover, this analytic model lends itself for nonlinear inversion—i.e., find the sets of parameters θ_i given $s(t)$.

Multiscale detection: Seismic traces as defined in Equation 1 are challenging because they violate most of the assumptions that underlay methods such as deconvolution. This is because the waveforms in Equation 1 are allowed to vary in a non-stationary fashion, which for a single source function, corresponds to an Earth whose transitions differ from ordinary step functions. The latter would justify deconvolution approaches such as spiky deconvolution to locate the reflectors. Instead, we opt to use maxima along the *Wavelet Transform Modulus Maxima Lines* (WTMMLs) (Mallat, 1997). We write the *complex wavelet transform* of a seismic trace s as a convolution product

$$\mathscr{W}s(t,\sigma) = \left(s * \bar{\psi}_\sigma\right)(t), \tag{2}$$

where $\bar{\psi}_\sigma(t) = \frac{1}{\sqrt{\sigma}}\psi^*(\frac{-t}{\sigma})$, and $\sigma \geq 0$ is the scale of wavelet ψ. Here, the symbol * denotes the complex conjugate. Following Mallat (1997), we define a WTMML as a connected curve, $\sigma(t)$, in the time-scale plane (t,σ), along which all points are modulus maxima. Singularities (events) are detected by finding the maximum point along each modulus maxima line (see Fig. 2(a)). These points yield approximate estimates for the scale (= bandwidth) and location of the reflection events. An initial approximation for the phase can be calculated from the complex wavelet coefficients as well. The advantage of this method is that very few assumptions are made regarding the type of reflected waveforms, making this approach a relatively robust event detector.

Segmentation: The result of the detection stage is a set of locations, scales, and phases— i.e., $\{(\tau^{(n)}, \sigma^{(n)}, \phi^{(n)}) \mid n = 1\cdots N\}$, where N is the number of detected maxima. We extract the n^{th} detected waveform by multiplying the seismic trace by a window function centered at $\tau^{(n)}$ and with a support proportional to $\sigma^{(n)}$ (see Fig. 2(b)). The output of this procedure consists of N signals with 'isolated' events $s^{(n)}(t)$. Even though this segmentation procedure is somewhat arbitrary, we found this method to perform reasonably well for cases where inter-event distances are not too small. Sub-wavelength details are not extracted and are left to the next estimation stage.

Nonlinear parametric inversion: To complete the characterization, we need to estimate the attributes of the individual waveforms—i.e., we need to estimate $\tilde{\theta}^{(n)}$ for each $n = 1\cdots N$ given $s^{(n)}(t)$. For this purpose, we solve N nonlinear least-squares problems

$$\tilde{\theta}^{(n)} = \arg\min_{\theta\in\Theta} \left\| s^{(n)} - M[\theta] \right\|_2^2 \quad \text{with} \quad n = 1\cdots N, \tag{3}$$

where $M[\theta] = \{f_\theta : \theta \in \Theta\}$ is the collection of all feasible waveforms—i.e., $\theta = [\tau, \sigma, \alpha, \phi] \in \Theta$ with Θ the set of feasible parameters. The set of estimated parameters $\tilde{\theta}^{(n)}$ signifies the attributes of the n^{th} event. We solve the above optimization problem with a quasi-Newton method (BFGS, Nocedal and Wright, 1999; Kelley, 1999). In Figure 2, we show an example of our waveform characterization method.

RELATION TO ROCK PHYSICS

At first glance, our exposé so far may leave the reader with the impression that we are merely interested in some mathematical technique without an obvious link to the (rock) physical processes that may be responsible for transitions other than zero- or first-order discontinuities. One can argue that the former models a major unconformity where two different rock types are in welded contact, whereas the second could arguably be used to model some transitional region, which leaves the fractional transitions without an obvious physical interpretation.

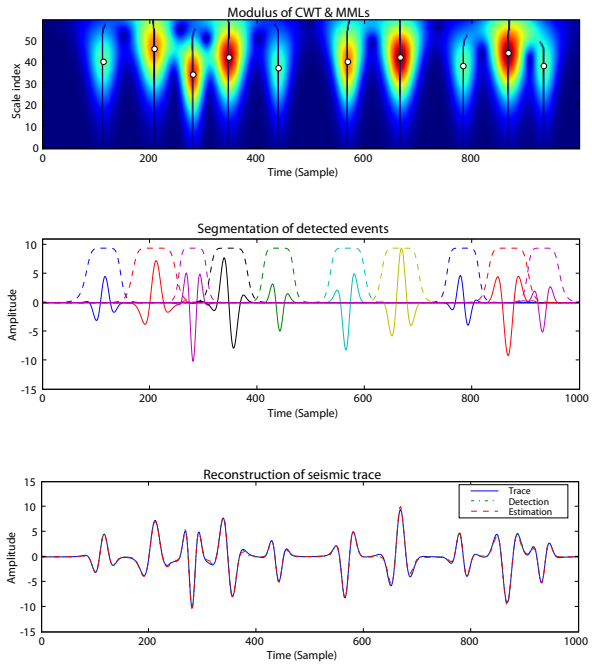

Figure 2: Seismic waveform characterization for a synthetic seismic trace. **(top)** Magnitude complex wavelet coefficients with warm colors corresponding to large magnitudes. The vertical and horizontal axes show scale and location, respectively. Dark blue lines show WTMML and white circles identify events. **(middle)** Segmentation of individual events (solid waveform) by using a window function (dashed line with same color) **(bottom)** Comparison between the reconstructed trace, formed by superposition of all characterized events, with the original seismic trace.

The site-percolation model: Variations in both the density of mass and bulk modulus determine the reflection of acoustic waves. Even though these properties appear on an equal footing in the acoustic impedance, their physical significance is very different. For bi-compositional mixtures, for instance, the density is trivially related to the volume fractions of the two rock components. This property does not hold for the bulk modulus, which depends on the microscopic arrangement of the two rock constituents. Upper- and lower bounds, such as Voigt and Reuss, are used to 'sandwich' all possible values for modulus for all possible arrangements. Unfortunately, this sort of formulation is smooth in the volume fraction—i.e., these bounds are smooth as observed in Figure 3 dashed lines. This smoothness implies a smooth depth dependence for volume fractions that increase linearly with depth and hence will not generate a specular reflection.

By bringing in the notion of connectivity, arguably important for elastic moduli, Herrmann and Bernabé (2004) proposed to use ideas from percolation theory, where this concept plays a central role. According to this model, the elastic moduli of a binary mixture change suddenly when the volume fraction, p of the stronger of the two materials connects. We illustrate this in Figure 3(a), where a connected cluster of strong (black) material is formed at some critical volume fraction. At that

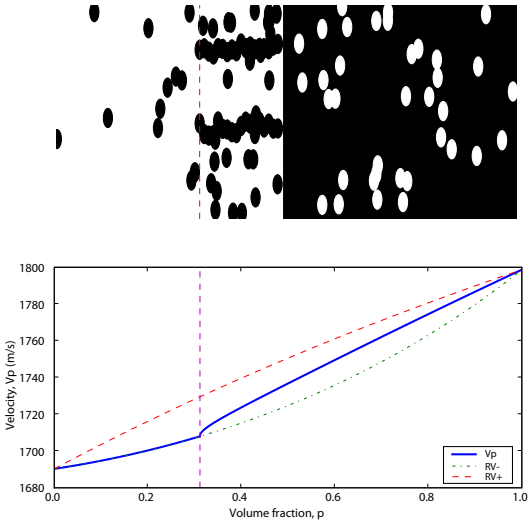

Figure 3: Schematic site-percolation model. The percolation threshold $p_c = p(z_c)$, which corresponds to a critical depth z_c, is denoted by a vertical dashed line. **(top)** Illustration of coexistence region. Black and white ellipsoids show inclusions of strong and weak materials, respectively. At critical volume fraction p_c (dashed vertical lines), strong material inclusions percolate and an infinite connected cluster is formed. **(bottom)** Corresponding compressional wave velocity (solid line) with a singularity at p_c as a function of volume fraction. It is bounded with Reuss and Voigt averages shown in dashed lines. The singularity order was taken to be $\beta = 0.41$.

point, an ∞-cluster of strong inclusions is formed. The volume fraction of the cluster for $p \geq p_c$ is given as $p^* = p\,(\frac{p-p_c}{1-p_c})^{\beta}$, where β is an exponent that depends on the type of percolation (see Herrmann and Bernabé (2004) for more details). Consequently, the bulk modulus, and hence the acoustic wavespeed, will have a β-order discontinuity (see Figure 3(b)). According to this model, the mixture's wavespeed for $p < p_c$ (and hence for shallower depth) follows the lower Reuss bound, to 'cusp up' to the upper Voigt bound for $p \geq p_c$—i.e., a β-order reflector emerges at a depth that corresponds to p_c. This cusp reflects and hence can be used to explain seismically observed transitions. However, since the exponents β predicted by percolation theory depend on several factors over which we have no control in this setting, we will have to use seismic images to estimate this exponent.

A CASE STUDY: OPAL-A TO OPAL-CT TRANSITION

To test whether the above model can be used to explain seismically observed waveforms, we submit a seismic subsection of the Faeroe-Shetland basin West of the Shetlands to our waveform characterization and we zoom in onto the opal-A to opal-CT transition that also contains a well constraint (Figure 4). Core samples taken from this borehole indicate that the strong event at $t = 2.9$ s is diagenetic and corresponds to an opal-A to opal-CT transition (Davies et al., 2001; Davies and Cartwright, 2002). Moreover, the samples were found to change in volume fraction for opal-CT from 10% at the top of the transition zone to 76% below the unconformity (Davies and Cartwright,

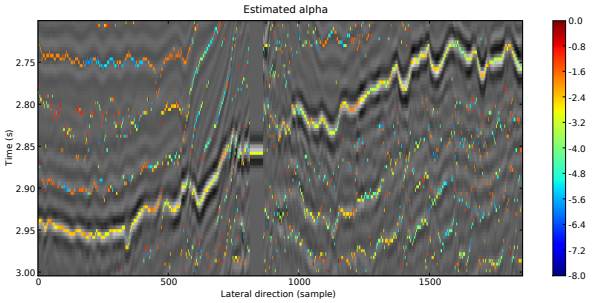

Figure 4: Seismic section including well tie. The locations of the colored dots corresponds to the estimated locations whereas the color corresponds to the estimated singularity order.

2002). If we assume a linear gradient for the volume fraction between these two values, we can use our site-percolation to model the shape of the transition as a function of depth. Since no sonic well data is available at this depth, we take representative values for the bulk modulus for both opal types from the literature (Guerin, 2000, logs measured in hole 904A).

At this point, we are in principle in a position to tie seismic to a waveform generated from our percolation model. Two pieces of the puzzle are still missing, namely the seismic source function and the order of discontinuity β. We estimate the seismic source function by taking the average over the estimated scale exponents from the sea-bottom reflector, which we assume to be close to zero-order. This procedure allows us to correct for the order of the seismic wavelet in additional to applying the unit shift between the order of the reflectivity and the bulk modulus. The second piece of the puzzle is solved by averaging the estimated exponents along the opal-A to opal-CT transition, which after correction for the source leads to an estimate of $\alpha = 0.79$. This estimate is close to the value of $\beta = 0.81$, which leads to the best trial-and-error match between the seismic in Figure 4 and our synthetic trace. We compute this trace using a convolution model, where the volume fraction of opal-CT is a proxy for depth or time. Figure 5 contains plots for the density, which is smooth, the compressional wavespeed, including the bounds, its derivative and the reflection coefficients. It is clear, that the wavespeed has a singularity at the critical depth.

DISCUSSION AND CONCLUSIONS

This paper is a first attempt towards a combination of sophisticated data inversion techniques with a rock-physical model that predicts the fine-structure of transitions as a function of the volume fraction for the stronger of the two components of a binary-rock mixture. Application of this methodology to the opal-A to opal-CT transition gives us the following insights. First, detailed information on the nature of transitions is reflected into waveforms. Second, this information can be characterized by first detecting the events by the multiscale wavelet transform, followed by a segmentation into individual waveforms and a subsequent parametric inversion. Third, repeated

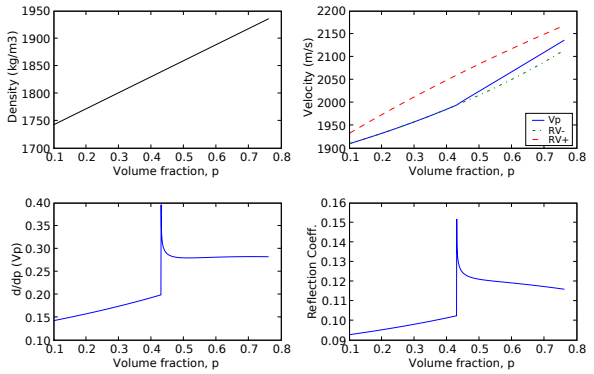

Figure 5: Modeled opal-A to opal-CT transition. Properties for opal-A are taken to be $\rho = 1713.90$ kg/m^3 and $V_p = 1889.65$ m/s. For opal-CT, density and P-wave velocity are assumed to be $\rho = 2006.06$ kg/m^3 and $V_p = 2237.71$ m/s, respectively. The density **(top left)** and P-wave velocity **(top right)** profiles are plotted as a function of volume fraction of opal-CT. The velocity is bounded by Reuss and Voigt averages and shows a critical point. This singularity is clearly visible from the derivative of the velocity **(bottom left)**, and can also be observed in the reflection coefficients **(bottom right)**.

application of this procedure to a seismic section leads to an attribute map where reflectors are overlaid with colored dots, which localize the positions of the transitions and whose color indicates their order. Fourth, with the estimate for the order parameter, a model for the transition can be built, yielding a waveform close to the seismically imaged waveform associated with the opal transition. This latest finding is particularly exciting since it gives an indication that the percolation model for the bulk modulus can be used to explain the details of waveforms associated with the opal transition. This means that sharp seismic reflectors can emerge even in cases where the composition of the rock seemingly changes smoothly. The onset of connectivity amongst the stronger of two mixing materials as function of the volume fraction is responsible for this sharp transition. This finding is new and encouraging and will help us to constrain unconformities from seismic and to better understand the processes responsible for transitions in the Earth's subsurface. In addition, our work may give us complementary information since the scale exponent associated with percolation depends on factors such as the type of mixing. This implies that our attribute maps may provide complementary information on changes along major unconformities.

Acknowledgments: The authors thank Chevron company for financially supporting the grant in aid ChaRM. We would also like to thank Veritas DGC for providing the dataset and additional information. Finally, we would like to thank Dave Wilkinson and Yves Bernabé for fruitful discussions. This work was in part financially supported by NSERC Discovery Grant 22R81254 and CRD Grant DNOISE 334810-05 of F. J. H.

REFERENCES

Blu, T. and M. Unser, 2003, A complete family of scaling functions: the (α, τ) fractional splines: Proceedings of the Twenty-Eighth IEEE International Conference on Acoustics, Speech, and Signal Processing (ICASSP'03), 505 – 508.

Davies, R. J. and J. Cartwright, 2002, A fossilized Opal A to Opal C/T transformation on the northeast Atlantic margin: support for a significantly elevated Palaeogeothermal gradient during the Neogene?: Basin Research, **14**, 467 – 486.

Davies, R. J., J. Cartwright, J. Pike, and C. Line, 2001, Early Oligocene initiation of North Atlantic Deep Water formation: Letters to Nature, **410**, 917 – 920.

Guerin, G., 2000, Acoustic and thermal characterization of oil migration, gas hydrates formation and silica diagenesis: PhD thesis, Columbia University.

Hashin, Z. and S. Shtrikman, 1962, On some variational principles in anisotropic and nonhomogeneous elasticity: Journal of the Mechanics and Physics of Solids, **10**, 335 – 342.

Herrmann, F. J., 2001, Singularity Characterization by Monoscale Analysis: Applications to Seismic Imaging: Applied and Computational Harmonic Analysis, **11**, 64 – 88.

———, 2005, Seismic deconvolution by atomic decomposition: A parametric approach with sparseness constraints: Integrated Computer-Aided Engineering, **12**, 69 – 91.

Herrmann, F. J. and Y. Bernabé, 2004, Seismic singularities at upper mantle discontinuities: a site percolation model: Geophysical Journal International, **159**, 949 – 960.

Herrmann, F. J., W. J. Lyons, and C. Stark, 2001, Seismic facies characterization by monoscale analysis: Geophysical Research Letters, **28**, 3781 – 3784.

Kelley, C. T., 1999, Iterative methods for optimization. Frontiers in Applied Mathematics, No. 18: SIAM.

Mallat, S., 1997, A wavelet tour of signal processing: Academic Press.

Nocedal, J. and S. J. Wright, 1999, Numerical optimization, 1st ed. Springer Series in Operations Research: Springer-Verlag.